Electronic Supplementary Information
for

Quantum Mechanical Effects in Acid-Base Chemistry

Computational Methods

PES computations

The potential energy surface (PES) computations were performed on the optimized structure of the complex (acetic acid dimer or acid-base complex) in gas phase. The scan of the PES was completed by computing the energy when the shared hydrogen atom was moved in steps of 0.02 Å along the line of the two heavy atoms involved in the hydrogen bond (nitrogen-oxygen or oxygen-oxygen atoms) by decrease either the H-N or H-O distance. In these PES computations, the distance between the two heavy atoms involved in the formation of the hydrogen bond and the two closest carbon atoms (see Scheme CM1) were keep fixed, and the dihedral angles of the methyl groups and the planes planarity of the complex was also constrained, while the positions of the rest of the atoms in the complex were optimized.

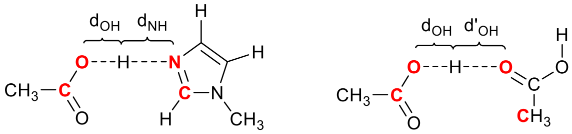

Scheme CM1. Structure of the complexes used to compute the PESs. The red highlighted atoms are the atoms whose position was constrained during the PES computation.

Setup and analyses of the AIMD simulations

AIMD simulations were performed for the mixtures of acetic acid and 1-methylimidazole at five concentrations of the acetic acid (X_{HA}). The systems were placed in cubic boxes with the periodic boundary conditions applied. The system size and box dimensions are summarized in Table S1.

Table S1. System setups for the AIMD simulations

	X_{HA}				
	0.02	0.67	0.86	0.99	1.00
Number of acetic acid	1	42	60	70	72
Number of 1-methylimidazole	51	21	10	1	0
Box length (Å)	19.0	19.0	19.3	18.9	19.2

From the AIMD simulations, we computed the self-diffusion coefficients (D) of acetic acid and 1-methylimidazole from the Einstein relation,

$$D = \lim_{t\to\infty} \frac{\langle |\boldsymbol{r}_i(t) - \boldsymbol{r}_i(0)|^2 \rangle}{6t}. \qquad \text{(S1)}$$

Here $\boldsymbol{r}_i(t)$ is the coordinate of the center of mass of molecule *i* at times t, and $\langle |\boldsymbol{r}_i(t) - \boldsymbol{r}_i(0)|^2 \rangle$ is the mean square displacement of the molecule. The diffusion coefficients were calculated from the linear region of the mean square displacement using the TRAVIS software.[1] The linear region depended on the length of the simulations, and was 7.3-14.5 ps, 5.3-10.5 ps, 15.0-30.0 ps, 15.3-30.6 ps and 6.1-12.2 ps for the solutions with X_{HA} of 1.00, 0.99, 0.86, 0.67 and 0.02, respectively. The resulting diffusion coefficients for the acid-base mixtures are listed in Table S2. The diffusion of the molecules is slower than that of liquid water ($D = 2.3 \times 10^{-9}$ m^2/s) at 298 K,[2] but is much faster than that of commonly observed ionic liquids. For example, the self-diffusion coefficients are 7.2×10^{-12} m^2/s and 5.2×10^{-12} m^2/s, respectively, for the cations and anions in the 1-butyl-3-methylimidazolium hexafluorophosphate ionic liquid at 298 K.[3]

Table S2. Self-diffusion coefficients (D) of acetic acid (HAc) and 1-methylimidazole (MIm) from the AIMD simulations of the acid-base mixtures

	X_{HA}				
	0.02	0.67	0.86	0.99	1.00
D of acetic acid (10^{-10} m^2/s)	12.5	5.3	6.7	8.2	11.9
D of 1-methylimidazole (10^{-10} m^2/s)	10.3	5.2	5.4	5.2	-

IR and NMR simulations details

The IR spectra of acetic acid, 1-methylimidazole and their mixture were calculated using the TRAVIS software.[1] A harmonic quantum correction factor, $Q = \frac{\beta\hbar\omega}{1-e^{-\beta\hbar\omega}}$, where β is the inverse temperature, was then applied to obtain the final spectra.[4]

The universal relation between the average ^{1}H NMR chemical shift and the proton position in short hydrogen bonds

$$\delta_H = 20.5 - 16.1\langle\nu\rangle^2, \qquad \text{(S3)}$$

was developed based on the observation that in a series of small molecules and the instantaneous ^{1}H NMR chemical shifts followed a general relation with the proton position, ν, [5]

$$\delta_H^{instantaneous} = 21.9 - 16.1\nu^2. \qquad \text{(S4)}$$

To evaluate whether Eq. S4 holds for the ionic solutions and validate Eq. S3 for the calculation of the ^{1}H NMR chemical shifts, we randomly extracted 500 clusters from the AIMD simulations of the acid-base mixture with X_{HA}=0.67. Each cluster contained a hydrogen bond pair between two acetic acids or between an acetic acid and a 1-methylimidazole with ν distributed between -1.0 Å and +1.0 Å. The cluster also contained all the acetic acid and 1-methylimidazole molecules within 5.5 Å of any atom of the hydrogen bond pair. The resulting clusters contained 103 – 202 atoms. The ^{1}H NMR chemical shift calculations were carried out using the Gauge-Independent Atomic Orbital method[6] with the B3LYP functional,[7] the D3 dispersion correction[8] and the 6-31+G(d,p) basis set using the Gaussian 16 software.[9] The chemical shift of 31.6 ppm for tetramethylsilane (TMS), which was calculated at the same level of theory, was subtracted to compute the instantaneous chemical shifts [5]. As shown in Fig. CM1, the instantaneous chemical shifts of the acid-base mixture follow the metric of Eq. S4 closely, hence validating our approach of using Eq. S3 for the chemical shift calculations.

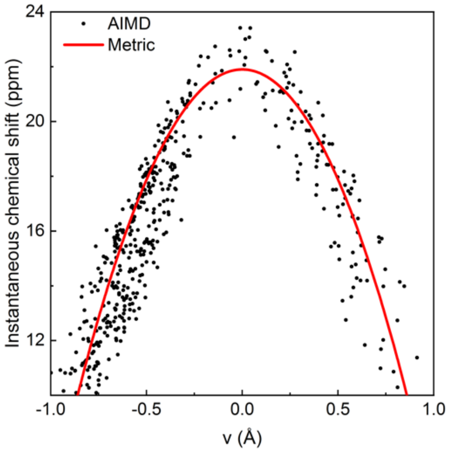

Fig. CM1. Comparison between the instantaneous ^{1}H NMR chemical shifts from the AIMD simulations of the acid-base mixture at X_{HA}=0.67 and the predictions from the metric in Eq. S4.

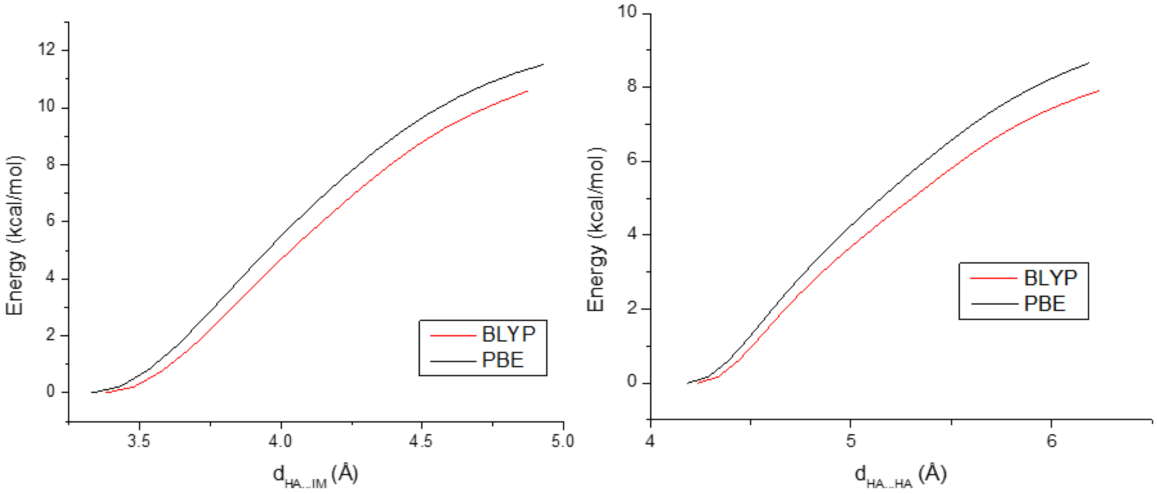

Fig. CM2. Comparison between the potential energy surfaces of the acetic acid dimer (left) and acetic acid 1-methylimidazole complex (right) in gas phase using different density functional. The potential energy surfaces are calculated using the BLYP-D2 and PBE-D2 methods and the 6-311++G(d,p) basis set.

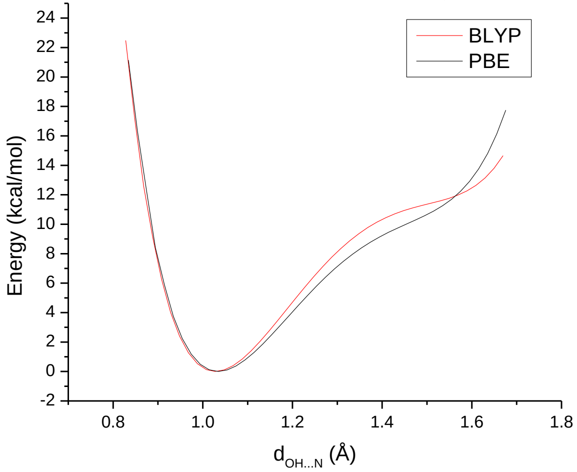

Fig. CM3. Comparison between the potential energy surfaces of the proton shuttling in the acetic acid and 1-methylimidazole complex from different density functionals and in gas phase. The calculations are performed using the BLYP-D2 and PBE-D2 methods and the 6-311++G(d,p) basis set.

Supplementary figures

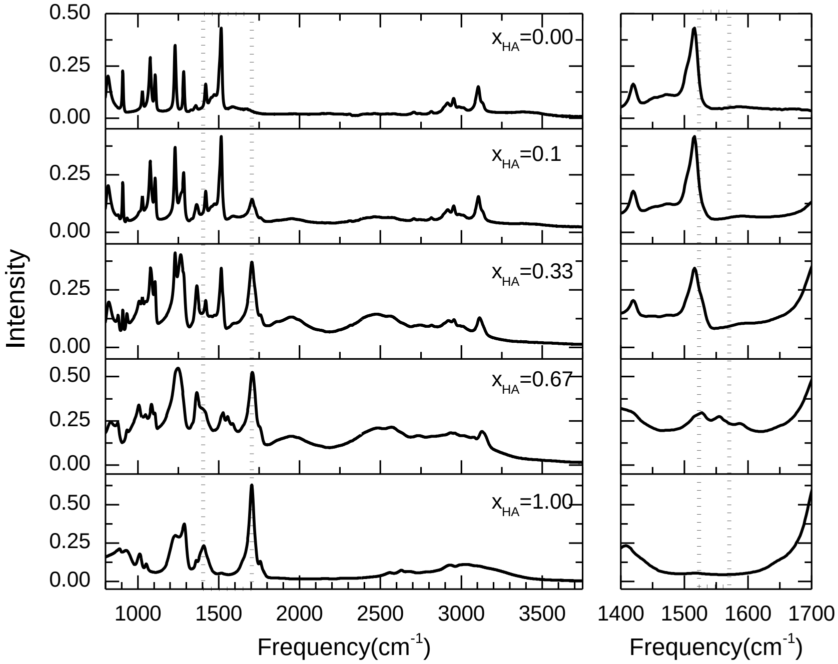

Fig. S1. ATR-FTIR spectra as a function of concentration (X_{HA}) for different mixtures of acetic acid and 1-methylimidazole in the region of 800-3000 cm^{-1} (left panels). The dashed area in the left panels showcases the carboxylate stretch region 1400-1700 cm^{-1}, which is expanded for easy visualization in the right panels. The dashed area in the right panels indicates the expected location for the carboxylate stretch region ~1560 cm^{-1} [10].

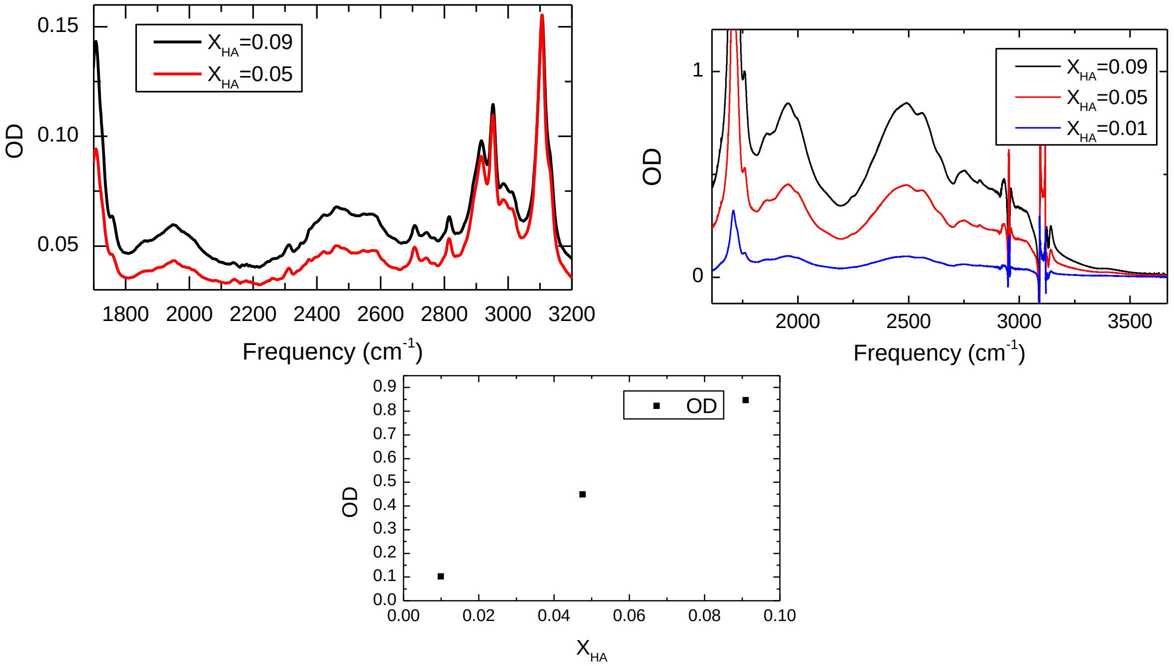

Fig. S2. ATR-FTIR spectra as a function of concentration (X_{HA}) for different mixtures of acetic acid and 1-methylimidazole (top left panel). FTIR transmission spectra as a function of the acid concentration (top right panel) and the dependence of the optical density for the maximum of the band at ~2500 cm^{-1} on the acid concentration (bottom panel).

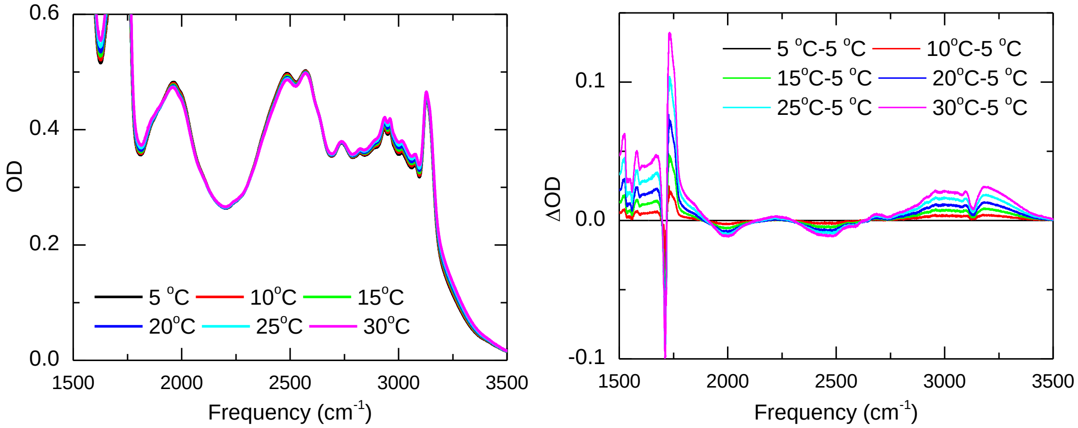

Fig. S3. Temperature dependent FTIR of the mixture of acetic acid and 1-methylimidazole for the molar fraction X_{HA}=0.86. Left panel shows the FTIR spectra at different temperatures and the right panel shows the difference spectra taking the 5°C data as a reference.

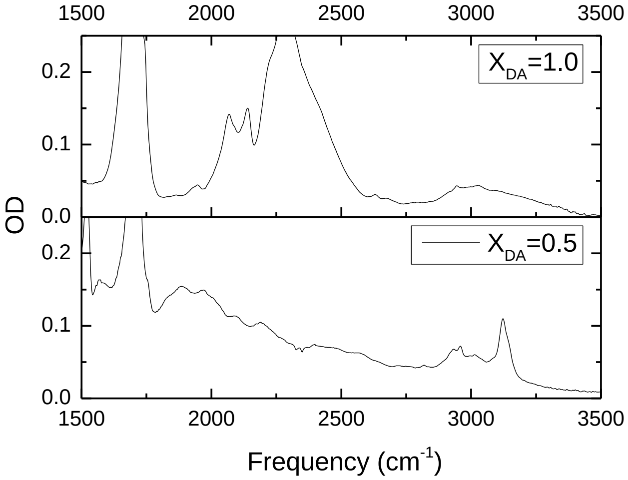

Figure S4. FTIR spectra of deuterated samples. Top and bottom panels show the spectra for pure acetic acid-d1 and the mixture of acetic acid-d1 and 1-methylimidazolium at the molar fraction of X_{DA}=0.5.

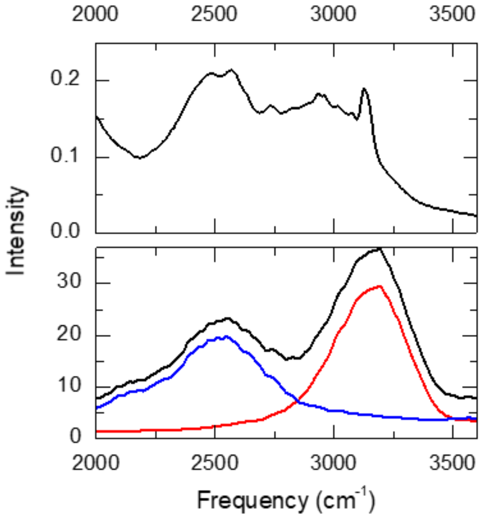

Figure S5. Comparison between the experimental and theoretical IR spectra. The experimental and theoretical spectra are shown in the top and bottom panels, respectively.

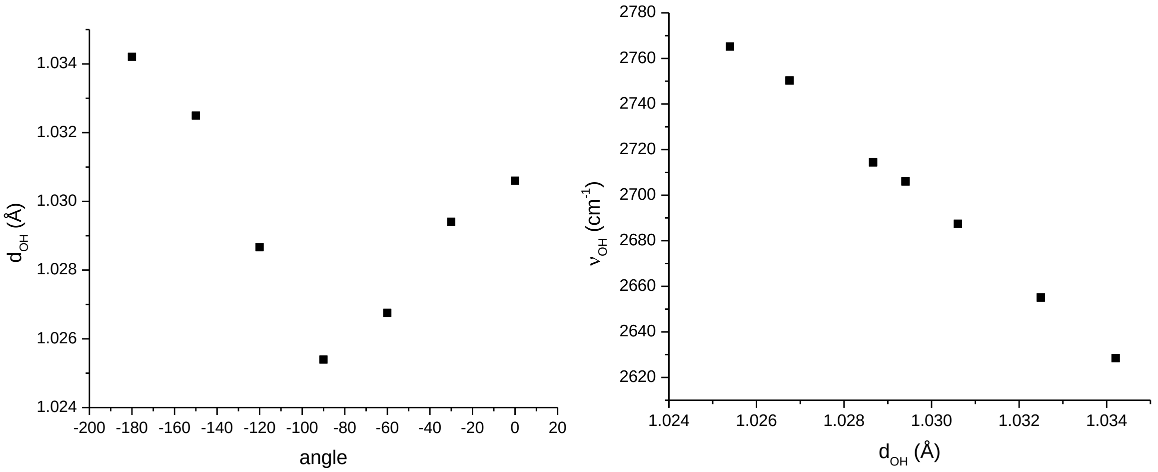

Figure S6. Distance between the H and O atoms of the acidic hydroxyl group as a function of the angle between the planes of acetic acid and 1-methylimidazole (left panel) and the frequency of the shuttling vibrational mode as a function of the O-H distance (right panel).

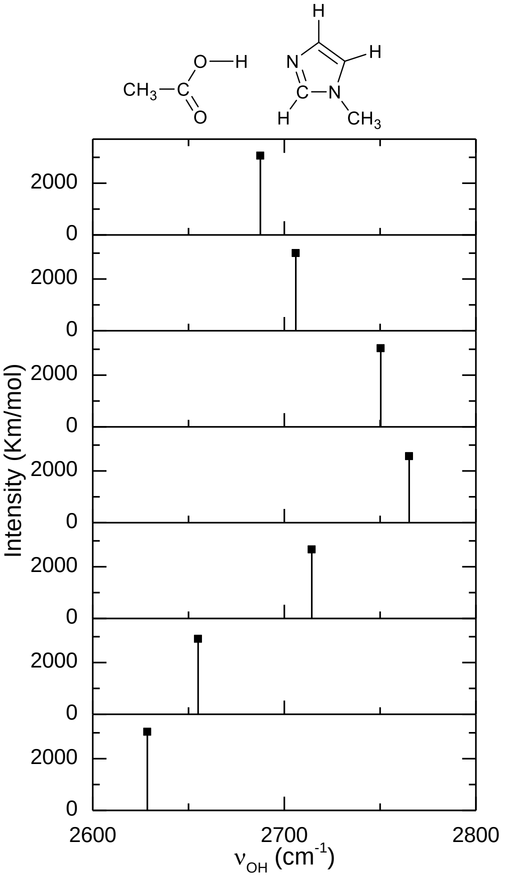

Figure S7. Angle dependence of the proton shuttling mode for the acetic acid-imidazole pair (left) and acetic acid with two imidazoles complex (right) from *ab initio* calculations.

References

1. M. Brehm, M. Thomas, S. Gehrke and B. Kirchner, *J. Chem. Phys.*, 2020, **152**, 164105.
2. M. Holz, S. R. Heil and A. Sacco, *Phys. Chem. Chem. Phys.*, 2000, **2**, 4740-4742.

3. H. Tokuda, K. Hayamizu, K. Ishii, M. Abu Bin Hasan Susan and M. Watanabe, *J. Phys. Chem. B*, 2004, **108**, 16593-16600.
4. S. A. Egorov, K. F. Everitt and J. L. Skinner, *J. Phys. Chem. A*, 1999, **103**, 9494-9499.
5. S. M. Zhou and L. Wang, *Phys. Chem. Chem. Phys.*, 2020, **22**, 4884-4895.
6. K. Wolinski, J. F. Hinton and P. Pulay, *J. Am. Chem. Soc.*, 1990, **112**, 8251-8260.
7. K. Raghavachari, *Theor. Chem. Acc.*, 2000, **103**, 361-363.
8. S. Grimme, J. Antony, S. Ehrlich and H. Krieg, *J. Chem. Phys.*, 2010, **132**, 154104.
9. M. J. Frisch, G. W. Trucks, H. B. Schlegel, G. E. Scuseria, M. A. Robb, J. R. Cheeseman, G. Scalmani, V. Barone, G. A. Petersson, H. Nakatsuji, X. Li, M. Caricato, A. V. Marenich, J. Bloino, B. G. Janesko, R. Gomperts, B. Mennucci, H. P. Hratchian, J. V. Ortiz, A. F. Izmaylov, J. L. Sonnenberg, Williams, F. Ding, F. Lipparini, F. Egidi, J. Goings, B. Peng, A. Petrone, T. Henderson, D. Ranasinghe, V. G. Zakrzewski, J. Gao, N. Rega, G. Zheng, W. Liang, M. Hada, M. Ehara, K. Toyota, R. Fukuda, J. Hasegawa, M. Ishida, T. Nakajima, Y. Honda, O. Kitao, H. Nakai, T. Vreven, K. Throssell, J. A. Montgomery Jr., J. E. Peralta, F. Ogliaro, M. J. Bearpark, J. J. Heyd, E. N. Brothers, K. N. Kudin, V. N. Staroverov, T. A. Keith, R. Kobayashi, J. Normand, K. Raghavachari, A. P. Rendell, J. C. Burant, S. S. Iyengar, J. Tomasi, M. Cossi, J. M. Millam, M. Klene, C. Adamo, R. Cammi, J. W. Ochterski, R. L. Martin, K. Morokuma, O. Farkas, J. B. Foresman and D. J. Fox, Gaussian, Inc., Wallingford, CT, 2016.
10. L. H. Jones and E. Mclaren, *J. Chem. Phys.*, 1954, **22**, 1796-1800.